Inclusive Jet Cross Section in $\bar{p}p$ Collisions at $\sqrt{s}=1.8$ TeV

F. Abe,[9] D. Amidei,[4] G. Apollinari,[16] M. Atac,[4] P. Auchincloss,[15] A. R. Baden,[6] N. Bacchetta,[11] M. W. Bailey,[14] A. Bamberger,[4],[a] P. de Barbaro,[15] B. A. Barnett,[8] A. Barbaro-Galtieri,[10] V. E. Barnes,[14] T. Baumann,[6] F. Bedeschi,[13] S. Behrends,[2] S. Belforte,[13] G. Bellettini,[13] J. Bellinger,[21] D. Benjamin,[20] J. Bensinger,[2] A. Beretvas,[4] J. P. Berge,[4] S. Bertolucci,[5] S. Bhadra,[7] M. Binkley,[4] D. Bisello,[11] R. Blair,[1] C. Blocker,[2] A. Bodek,[15] V. Bolognesi,[13] A. W. Booth,[4] C. Boswell,[8] G. Brandenburg,[6] D. Brown,[6] E. Buckley-Geer,[17] H. S. Budd,[15] G. Busetto,[11] A. Byon-Wagner,[4] K. L. Byrum,[21] C. Campagnari,[3] M. Campbell,[3] A. Caner,[4] R. Carey,[6] W. Carithers,[10] D. Carlsmith,[21] J. T. Carroll,[4] R. Cashmore,[4],[a] A. Castro,[11] F. Cervelli,[13] K. Chadwick,[4] G. Chiarelli,[5] W. Chinowsky,[10] S. Cihangir,[4] A. G. Clark,[4] M. Cobal,[13] D. Connor,[12] M. Contreras,[3] J. Cooper,[4] M. Cordelli,[5] D. Crane,[4] M. Curatolo,[5] C. Day,[4] F. DeJongh,[4] S. Dell'Agnello,[13] M. Dell'Orso,[13] L. Demortier,[2] B. Denby,[4] P. F. Derwent,[3] T. Devlin,[17] D. DiBitonto,[18] M. Dickson,[15] R. B. Drucker,[10] K. Einsweiler,[10] J. E. Elias,[4] R. Ely,[10] S. Eno,[3] S. Errede,[7] B. Esposito,[5] A. Etchegoyen,[4],[a] B. Flaugher,[4] G. W. Foster,[4] M. Franklin,[6] J. Freeman,[4] H. Frisch,[3] T. Fuess,[4] Y. Fukui,[9] A. F. Garfinkel,[14] A. Gauthier,[7] S. Geer,[4] D. W. Gerdes,[3] P. Giannetti,[13] N. Giokaris,[16] P. Giromini,[5] L. Gladney,[12] M. Gold,[10] K. Goulianos,[16] H. Grassmann,[11] G. M. Grieco,[13] C. Grosso-Pilcher,[3] C. Haber,[10] S. R. Hahn,[4] R. Handler,[21] K. Hara,[19] B. Harral,[12] R. M. Harris,[4] J. Hauser,[4] C. Hawk,[17] T. Hessing,[18] R. Hollebeek,[12] P. Hu,[17] B. Hubbard,[10] B. T. Huffman,[14] R. Hughes,[12] P. Hurst,[5] J. Huth,[4] J. Hylen,[4] M. Incagli,[13] T. Ino,[19] H. Iso,[19] H. Jensen,[4] C. P. Jessop,[6] R. P. Johnson,[4] U. Joshi,[4] R. W. Kadel,[10] T. Kamon,[18] S. Kanda,[19] D. A. Kardelis,[7] I. Karliner,[7] E. Kearns,[6] L. Keeble,[18] R. Kephart,[4] P. Kesten,[2] R. M. Keup,[7] H. Keutelian,[4] D. Kim,[4] S. Kim,[19] L. Kirsch,[2] K. Kondo,[19] J. Konigsberg,[6] E. Kovacs,[4] S. E. Kuhlmann,[1] E. Kuns,[17] A. T. Laasanen,[14] J. I. Lamoureux,[21] S. Leone,[13] J. Lewis,[4] W. Li,[1] T. M. Liss,[7] P. Limon,[4] N. Lockyer,[12] M. Loreti,[11] E. H. Low,[12] C. B. Luchini,[7] P. Lukens,[4] P. Maas,[21] M. Mangano,[13] J. P. Marriner,[4] M. Mariotti,[13] R. Markeloff,[21] L. A. Markosky,[21] R. Mattingly,[2] P. McIntyre,[18] A. Menzione,[13] T. Meyer,[18] S. Mikamo,[9] M. Miller,[3] T. Mimashi,[19] S. Miscetti,[5] M. Mishina,[9] S. Miyashita,[19] Y. Morita,[19] S. Moulding,[2] J. Mueller,[17] A. Mukherjee,[4] L. F. Nakae,[2] I. Nakano,[19] C. Nelson,[4] C. Newman-Holmes,[4] J. S. T. Ng,[6] M. Ninomiya,[19] L. Nodulman,[1] S. Ogawa,[19] R. Paoletti,[13] V. Papadimitriou,[4] A. Para,[4] G. Pauletta,[13] E. Pare,[6] S. Park,[4] J. Patrick,[4] L. Pescara,[11] T. J. Phillips,[6] R. Plunkett,[4] L. Pondrom,[21] J. Proudfoot,[1] F. Ptohos,[6] G. Punzi,[13] D. Quarrie,[4] K. Ragan,[12] G. Redlinger,[3] J. Rhoades,[21] M. Roach,[20] F. Rimondi,[4],[a] L. Ristori,[13] T. Rodrigo,[4] T. Rohaly,[12] A. Roodman,[3] W. K. Sakumoto,[15] A. Sansoni,[5] R. D. Sard,[7] A. Savoy-Navarro,[4] V. Scarpine,[7] P. Schlabach,[6] E. E. Schmidt,[4] O. Schneider,[10] M. H. Schub,[14] R. Schwitters,[6] A. Scribano,[13] S. Segler,[4] Y. Seiya,[19] M. Shapiro,[10] N. M. Shaw,[14] M. Sheaff,[21] M. Shochet,[3] J. Siegrist,[10] P. Sinervo,[12] J. Skarha,[8] K. Sliwa,[20] D. A. Smith,[13] F. D. Snider,[8] L. Song,[12] M. Spahn,[10] P. Sphicas,[4] R. St. Denis,[6] A. Stefanini,[13] G. Sullivan,[3] R. L. Swartz, Jr.,[7] M. Takano,[19] F. Tartarelli,[13] K. Takikawa,[19] S. Tarem,[2] D. Theriot,[4] M. Timko,[18] P. Tipton,[4] S. Tkaczyk,[4] A. Tollestrup,[4] J. Tonnison,[14] W. Trischuk,[6] N. Turini,[13] Y. Tsay,[3] F. Ukegawa,[19] D. Underwood,[1] S. Vejcik, III,[8] R. Vidal,[4] R. G. Wagner,[1] R. L. Wagner,[4] N. Wainer,[4] J. Walsh,[12] T. Watts,[17] R. Webb,[18] C. Wendt,[21] H. Wenzel,[13] W. C. Wester, III,[10] T. Westhusing,[13] S. N. White,[16] A. B. Wicklund,[1] H. H. Williams,[12] B. L. Winer,[15] J. Wyss,[11] A. Yagil,[4] K. Yasuoka,[19] G. P. Yeh,[4] J. Yoh,[4] M. Yokoyama,[19] J. C. Yun,[4] A. Zanetti,[13] F. Zetti,[13] and S. Zucchelli[4],[a]

(CDF Collaboration)

[1]*Argonne National Laboratory, Argonne, Illinois 60439*
[2]*Brandeis University, Waltham, Massachusetts 02254*
[3]*University of Chicago, Chicago, Illinois 60637*
[4]*Fermi National Accelerator Laboratory, Batavia, Illinois 60510*
[5]*Laboratori Nazionali di Frascati, Istituto Nazionale di Fisica Nucleare, Frascati, Italy*
[6]*Harvard University, Cambridge, Massachusetts 02138*

 © 1992 The American Physical Society

[7]*University of Illinois, Urbana, Illinois 61801*
[8]*The Johns Hopkins University, Baltimore, Maryland 21218*
[9]*National Laboratory for High Energy Physics (KEK), Tsukuba, Ibaraki 305, Japan*
[10]*Lawrence Berkeley Laboratory, Berkeley, California 94720*
[11]*Universita di Padova, Istituto Nazionale di Fisica Nucleare, Sezione di Padova, I-35131 Padova, Italy*
[12]*University of Pennsylvania, Philadelphia, Pennsylvania 19104*
[13]*Istituto Nazionale di Fisica Nucleare, University and Scuola Normale Superiore of Pisa, I-56100 Pisa, Italy*
[14]*Purdue University, West Lafayette, Indiana 47907*
[15]*University of Rochester, Rochester, New York 14627*
[16]*Rockefeller University, New York, New York 10021*
[17]*Rutgers University, Piscataway, New Jersey 08854*
[18]*Texas A&M University, College Station, Texas 77843*
[19]*University of Tsukuba, Tsukuba, Ibaraki 305, Japan*
[20]*Tufts University, Medford, Massachusetts 02155*
[21]*University of Wisconsin, Madison, Wisconsin 53706*
(Received 7 August 1991)

We present a measurement of the inclusive jet cross section in $\bar{p}p$ collisions at $\sqrt{s}=1.8$ TeV at the Fermilab Tevatron using the Collider Detector at Fermilab. Good agreement is seen with the predictions of recent next-to-leading-order $[O(\alpha_s^3)]$ QCD predictions. The dependence of the cross section on clustering cone size is reported for the first time. An improved limit on Λ_c, a term characterizing possible quark substructure, is set at 1.4 TeV (95% C.L.).

PACS numbers: 13.87.Ce, 12.38.Qk, 13.85.Ni

Recently, calculations of the inclusive jet cross section, $\sigma(\bar{p}p\rightarrow \text{jet}+X)$, have become available at next-to-leading order $[O(\alpha_s^3)]$ [1-3]. The new QCD predictions explicitly include jet definitions at the parton level which can be directly related to experimental jet algorithms. This property allows a comparison of the jet cross section to theory for different effective jet sizes, and is not a feature of the leading-order $[O(\alpha_s^2)]$ calculation. In addition, a reduction of both experimental and theoretical uncertainties has improved the precision of the comparison of data to QCD. The theoretical uncertainty associated with unknown higher-order contributions is typically estimated from the sensitivity of the calculated cross section to the choice of scale μ used for evaluating the strong coupling constant $\alpha_s(\mu)$ and for the evolution of the parton distribution functions. Using this as a measure of the precision of the theory, the uncertainty at $O(\alpha_s^3)$ is 5 to 10 times smaller than the uncertainty at $O(\alpha_s^2)$ [4]. A data sample of 4.2 pb^{-1} from an extended run of the Fermilab Tevatron $\bar{p}p$ Collider has given a measurement of the inclusive jet cross section over 7 orders of magnitude, from 35 to 450 GeV in transverse energy.

The CDF detector has been described in detail elsewhere [5]. The detector elements most relevant to this study are the central calorimeters, which cover the pseudorapidity range $|\eta|\leq 1.1$ [$\eta\equiv -\ln\tan(\theta/2)$ and θ is the polar angle with respect to the beam]. These calorimeters are segmented into projective towers of $\Delta\eta\times\Delta\phi=0.1\times0.26$ (ϕ in radians). The detector was triggered by the presence of a localized cluster of transverse energy in the calorimeter. A trigger cluster is initiated by a "seed" tower above 3 GeV and consists of all contiguous towers in η and ϕ above 1 GeV. In order to span a large range of cross sections, three separate thresholds were imposed on the transverse energy E_t of the trigger clusters, 20, 40, and 60 GeV. The 20 and 40 GeV triggers were prescaled to accept 1 in 300 and 1 in 30 events, respectively.

Jets were identified using a cone algorithm, described fully in [6]. Jet clusters were formed by including all towers with $E_t > 100$ MeV inside a cone of radius $R=[(\Delta\eta)^2+(\Delta\phi)^2]^{1/2}$. Jet energy E was determined using a scalar sum of tower energies in the cone. E_t was taken as $E\sin\theta$, where θ was taken from the angle between a line drawn from the cluster center to the event-vertex position and the beam line. The above algorithm is very similar to the jet definition employed at the parton level in producing the $O(\alpha_s^3)$ predictions for comparison [3]. The jets were clustered using three different radii, $R=0.4$, 0.7, and 1.0, to examine the R dependence.

The event vertex was required to be within 60 cm of the center of the detector along the beam line. In order to ensure a triggering efficiency for clusters greater than 98%, thresholds were placed on the minimum off-line cluster E_t for each trigger. These were 35, 60, and 100 GeV for the 20, 40, and 60 GeV triggers, respectively. The cuts were higher than the E_t of the trigger due to the differences in the off-line and trigger clustering. Backgrounds from cosmic-ray bremsstrahlung were rejected with better than 99.5% efficiency using criteria nearly identical to those described in Ref. [7]. Finally, jets in the sample were required to have $0.1\leq|\eta|\leq 0.7$ to ensure uniform detector response and containment of most of the jet energy in the central detector.

The measured jet E_t spectrum is distorted due to several effects. First, the low-energy response of the calorimeter to single hadrons is nonlinear, but is linear for photons and electrons. The jet energy measured in the calorimeter is a convolution of the single-particle response with the jet fragmentation spectrum. This, when combined with energy losses in uninstrumented regions, can give rise to a mean response that is typically less than the true jet energy. Second, the effect of the broad jet energy resolution on a steeply falling spectrum distorts the measured spectrum. The rms resolution for jets in the range $35 \leq E_t \leq 450$ GeV can be approximated by $\sigma_{\text{rms}} = 0.1E_t + 1$ GeV. The absence of a $\sqrt{E}$ behavior for the resolution is due mostly to the presence of long tails in the jet response function associated with energy loss in uninstrumented regions (cracks). Finally, the underlying event not associated with the hard scattering process can contribute energy to the clustering cone which should not be included in the jet energy. The average E_t density (uncorrected for nonlinearities) from the underlying event was measured in regions of the calorimeter far from jet clusters and was approximately 1.2 ± 0.3 GeV per unit area in the η-ϕ plane (ϕ in radians). No energy corrections were applied for energy falling outside of the clustering cone, as this, in principle, should be taken into account by the next-to-leading-order calculations [2,3,8].

The effects of resolution smearing and energy losses on the jet spectrum were determined and corrected using the following procedure. The response of the calorimeter to pions between 0.5 and 227 GeV was determined from test beam data and isolated tracks in the central tracking chamber. The jet fragmentation spectrum was also measured using charged tracks [9]. A Monte Carlo simulation incorporating both calorimeter response (nonlinearity, cracks, etc.) and tuned Field-Feynman [10,11] jet fragmentation was used to determine energy losses and resolution for jets in the E_t range 10 to 500 GeV. Average energy loss is 17% (12%) at 35 (300) GeV, with calorimeter response to hadrons dominating. Next, a simultaneous unfolding of the raw jet spectrum for the two effects of energy loss and resolution was performed. This provided corrections to both the E_t and cross-section axes. Corrections to E_t and cross section at 35 (300) GeV are 7% and 20% (10% and 5%).

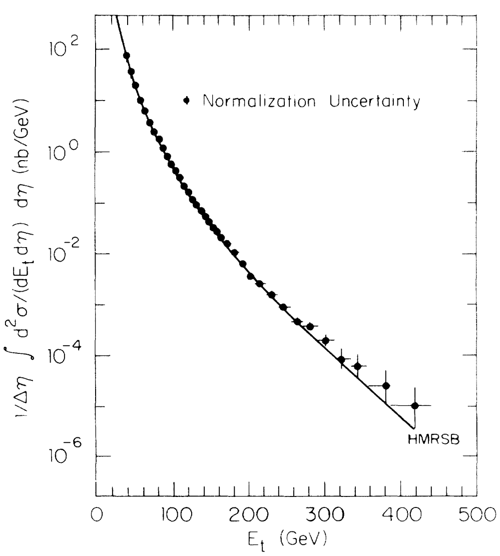

FIG. 1. Inclusive E_t spectrum for a cone size of $R = 0.7$, averaged over the pseudorapidity interval $0.1 \leq |\eta| \leq 0.7$. The curve represents the predictions of a next-to-leading-order QCD calculation by Ellis, Kunszt, and Soper [3]. The error bars on the data represent statistical and E_t-dependent systematic errors. An overall normalization uncertainty is also indicated.

We assign systematic uncertainties to the data based on our knowledge of detector effects and jet fragmentation. The largest uncertainties come from the modeling of the calorimeter response [12]. Because of the steeply falling E_t spectrum, a small error in energy scale can generate large uncertainties in the cross section. For values of jet E_t above 80 GeV, the uncertainty in the cross section, dominated by the determination of the absolute energy scale, is typically 22%. Below 80 GeV, systematic effects associated with jet energy resolution and the unsmearing procedure give an uncertainty in the cross section as high as 60%. These uncertainties are smaller than those reported in previous measurements of the jet cross section [6,13].

The cross section for a clustering radius $R = 0.7$ is shown in Fig. 1 along with a prediction from next-to-leading-order QCD [3] using the Harriman-Martin-Roberts-Stirling (HMRS) set B [14] parton distribution functions, with the renormalization-scale choice $\mu = E_t$. The data are presented as an average over the pseudorapidity interval $0.1 \leq |\eta| \leq 0.7$. The predictions and the data show good agreement over 7 orders of magnitude of cross section and E_t ranging from 35 to 450 GeV. In Fig. 2 the ratio of (data − theory)/theory is plotted for $R = 0.7$ to show the level of agreement on a linear scale. The $O(\alpha_s^3)$ calculation using the HMRS set B parton distribution function serves as a reference (i.e., is zero in Fig. 2). In Fig. 2(a), a range of $O(\alpha_s^3)$ and $O(\alpha_s^2)$ predictions are shown by varying the renormalization scale from E_t to $E_t/4$ to display the reduction in theoretical uncertainty at the next-to-leading order. To illustrate the variation associated with different parton distribution functions [Fig. 2(b)], we show curves from other parametrizations [14,15]. All normalizations in Figs. 1 and 2 are absolute. E_t-dependent systematic uncertainties are included in the error bars; the E_t-independent uncertainty is indicated in Fig. 2(b) as the horizontal dashed lines. The E_t-dependent systematic uncertainties, which dominate at $E_t \leq 150$ GeV, are highly correlated from point to point.

We have made a quantitative comparison of the data to the $O(\alpha_s^3)$ predictions by introducing a floating normalization constant. A χ^2 was minimized which takes into account the correlations due to the systematic uncertainties. The fit was performed for $E_t \geq 80$ GeV where the uncertainties are smaller. Here recent parton distribution functions HMRS (B and E) [14] and Morfin and Tung (MT) (B and S) [15] were used. The best-fit normalization constants were 1.15, 1.13, 1.27, and 1.29 for HMRS sets B and E and MT sets S and B, respectively. The deviation of the normalizations from unity is of the same

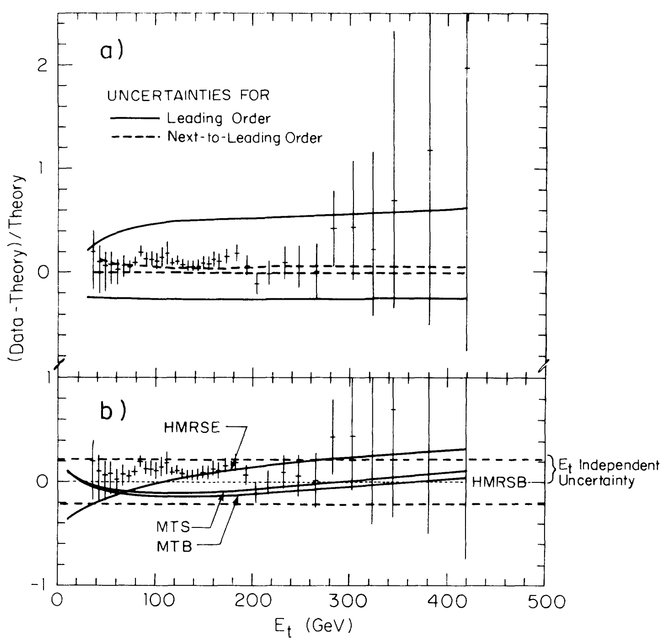

FIG. 2. The inclusive jet E_t spectrum for $R=0.7$ compared to theory as the ratio of (data − theory)/theory. The upper plot (a) illustrates the theoretical uncertainty associated with variation of the renormalization scale μ ($E_t \geq \mu \geq E_t/4$) for both leading order and next-to-leading order. The data have both the statistical and the E_t-dependent parts of the systematic uncertainties indicated. The lower plot (b) illustrates the dependence on the choice of parton distribution function. The $O(\alpha_s^3)$ prediction using the HMRS set B [14] structure function is used as a reference.

magnitude as the experimental uncertainty ($\approx 20\%$) on the cross section. The confidence levels associated with the fits were 19%, 0.1%, 49%, and 56%, respectively, for the above sets of parton distribution functions and 30 degrees of freedom. HMRS set B and MT sets S and B give acceptable fits, while the shape of HMRS set E is inconsistent, mostly in the region between 80 and 250 GeV.

The variation of the jet cross section as a function of clustering radius R is shown in Fig. 3 for jets of 100 GeV E_t, along with $O(\alpha_s^3)$ predictions (MRS B [16] parton distribution functions) with three different choices of renormalization scale μ. Only statistical errors have been plotted with the data, but there is an additional $\approx 23\%$ systematic uncertainty which is strongly correlated from point to point. The curves represent the typical theoretical uncertainty in the R dependence of the cross section and exhibit a smaller uncertainty near $R=0.7$ than for other values of R. We fit the data with a function favored by theory [8], $A+B\ln R$, where A and B are free parameters, and we compare the slope at $R=0.7$ to theoretical predictions. The result of the fit is $A=0.79\pm0.02$ nb/GeV and $B=0.49\pm0.03$ nb/GeV. The fit takes into account the correlations associated with the experimental systematic uncertainties. The derivative of this function with respect to R, evaluated at $R=0.7$, is

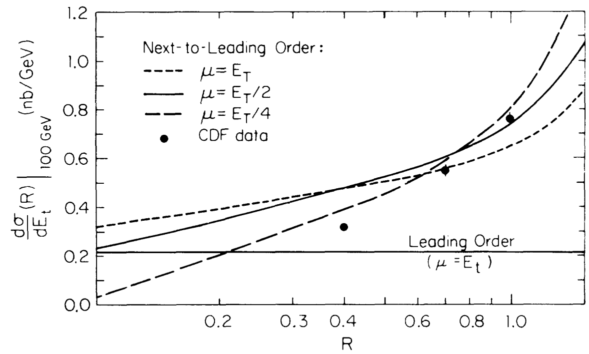

FIG. 3. The variation of jet cross section with clustering cone size R for jets of 100 GeV E_t. Statistical errors only are plotted on the data points. An overall, R-independent systematic uncertainty of 23% has not been indicated. The curves represent a range of theoretical predictions associated with different choices of renormalization scale μ using the MRS B [16] parton distribution function.

0.70 ± 0.05 nb/GeV and compares reasonably to an $O(\alpha_s^3)$ prediction of 0.5 ± 0.2 nb/GeV [17,18].

The presence of quark substructure can appear as an enhancement of the cross section at high E_t. This effect is conventionally parametrized in terms of a contact term of unit strength between left-handed quarks, characterized by the constant Λ_c with units of energy [19]. In order to search for quark substructure, predictions for the inclusive E_t spectrum for different parton distribution functions and values of Λ_c have been compared to the data. Only leading-order $[O(\alpha_s^2)]$ calculations that include this contact term are available at present. Because of this, we have fitted the data using a cone of $R=1.0$ to minimize the effects of energy outside the cone. The fits are performed by normalizing the predictions to the data using an overall multiplicative factor in the region $80 \leq E_t \leq 160$ GeV, where contributions from the contact term for $\Lambda_c \geq 750$ GeV are negligible. The fitted curves are then extrapolated to the region $E_t \geq 160$ GeV where they are compared to the data. The comparison takes into account Poisson statistics for bins with a small number of entries, and also the correlations associated with systematic uncertainties. We have used only recent sets of structure functions for this test (HMRS sets B and E and MT sets S and B) [14,15]. The HMRS set E was excluded due to poor fits in the normalization region. A lower limit of 1.4 TeV is set on Λ_c at the 95% confidence level. This represents the most conservative limit from the above structure functions (HMRS set B). The largest contribution to the χ^2 in this limit comes from the region $200 \leq E_t \leq 300$ and the absence of events above 420 GeV. This is a substantial improvement over the previously published limits of 750 [6] and 825 GeV [20].

To summarize, we have measured the inclusive jet cross section in $\bar{p}p$ collisions at $\sqrt{s}=1.8$ TeV. The data span 7 orders of magnitude in cross section, and include the highest values of E_t measured to date, allowing a stringent test of both higher-order QCD and possible quark substructure. Next-to-leading-order QCD calculations give a reasonable description of the data. The variation of jet cross section with clustering radius R is consistent with a next-to-leading-order $[O(\alpha_s^3)]$ calculation [3]. Finally a search for possible quark substructure has given a lower limit of 1.4 TeV (95% C.L.) on the compositeness energy scale Λ_c.

We thank the Fermilab accelerator division and the technical staffs of the participating institutions for their invaluable contributions. This work is supported in part by the U.S. Department of Energy and National Science Foundation, the Italian Istituto Nazionale di Fisica Nucleare, the Ministry of Science, Culture and Education of Japan, and the Alfred P. Sloan Foundation. We also wish to thank S. Ellis, M. Greco, P. Guillet, Z. Kunszt, and D. Soper for useful discussions and for providing results of their calculations.

[a] Visitor.

[1] R. Ellis, and J. Sexton, Nucl. Phys. **B269**, 445 (1986).
[2] F. Aversa *et al.*, Phys. Lett. B **210**, 225 (1988).
[3] S. Ellis, Z. Kunszt, and D. Soper, Phys. Rev. Lett. **62**, 2188 (1989); Phys. Rev. Lett. **64**, 2121 (1990).
[4] S. Ellis, Z. Kunszt, and D. Soper, in *Proceedings of the 1990 Meeting of the Division of Particles and Fields of the American Physical Society, Houston, 1990*, edited by W. Bonner and H. Miettinen (World Scientific, Singapore, 1990), p. 603.
[5] CDF Collaboration, F. Abe *et al.*, Nucl. Instrum. Methods Phys. Res., Sect. A **271**, 387 (1988).
[6] F. Abe *et al.*, Fermilab Report No. FNAL PUB 91/181, 1991 [Phys. Rev. D (to be published)].
[7] CDF Collaboration, F. Abe *et al.*, Phys. Rev. Lett. **62**, 613 (1989).
[8] S. Ellis, in Proceedings of the Snowmass 1990 High Energy Physics Workshop, Research Directions for the Decade [Department of Energy Report No. DOE/ER/4043-27, 1991 (to be published)].
[9] F. Abe *et al.*, Phys. Rev. Lett. **65**, 968 (1990).
[10] R. Field and R. Feynman, Nucl. Phys. **B136**, 1 (1978).
[11] F. Paige and S. Protopopescu, Brookhaven National Laboratory Report No. BNL-38034, 1986 (unpublished); in *Proceedings of the 1986 Summer Study on the Physics of the Superconducting Supercollider*, edited by R. Donaldson and J. Marx (Fermilab, Batavia, IL, 1986), p. 320.
[12] J. Huth, in *Proceedings of the Workshop on Calorimetry for the SSC, Tuscaloosa, Alabama, 1989*, edited by R. Donaldson and G. Gilchriese (World Scientific, Singapore, 1990).
[13] UA2 Collaboration, J. A. Appel *et al.*, Phys. Lett. **160B**, 349 (1985).
[14] P. Harriman, A. Martin, R. Roberts, and W. Stirling, Rutherford Laboratory Report No. RAL-90-007, 1990 (to be published).
[15] J. Morfin and W. K. Tung, Fermilab Report No. Fermilab-Pub-90/74, 1990 (to be published).
[16] A. Martin, R. Roberts, and W. Stirling, Phys. Rev. D **37**, 1161 (1988).
[17] S. Ellis, Z. Kunszt, and D. Soper (private communication).
[18] This issue has also been discussed by F. Aversa *et al.*, Z. Phys. C **49**, 459 (1991).
[19] E. Eichten, K. Lane, and M. Peskin, Phys. Rev. Lett. **50**, 811 (1983).
[20] UA2 Collaboration, J. Alitti *et al.*, Phys. Lett. B **257**, 232 (1991).